Available online at www.sciencedirect.com

ScienceDirect

Procedia Manufacturing 53 (2021) 348–358

Procedia MANUFACTURING

www.elsevier.com/locate/procedia

49th SME North American Manufacturing Research Conference, NAMRC 48, Ohio, USA

Optimizing the Expected Utility of Shape Distortion Compensation Strategies for Additive Manufacturing

Nathan Decker* and Qiang Huang

Department of Industrial and Systems Engineering, University of Southern California. 3715 McClintock Ave, GER 240, Los Angeles, CA 90089-0193, USA

* Corresponding author. Tel.: +1-213-740-4893; fax: +1-213-740-1120. *E-mail address:* ndecker@usc.edu

Abstract

In the past two decades, the field of additive manufacturing (AM) has seen tremendous growth, especially in the production of functional parts. Unfortunately, improving the dimensional accuracy of these printed parts to the point where they can be used for a broad range of applications has proven challenging. Several methodologies to improve the dimensional accuracy of 3D printed parts have been proposed in the literature. One approach that has seen a considerable amount of work in recent years is product design adjustment based on predictive modeling. Under this approach, predictions of geometric deviations across the surface of a part are used to modify the shape of a part before printing so as to counteract or compensate for the predicted deviations. However, a majority of compensation methods aim at minimizing expected geometric and dimensional error, with a lack of consideration of cost and uncertainty. This study presents a new strategy based on multi-attribute utility theory to account for cost and inherent uncertainty associated with a compensation decision. By establishing manufacturer preferences and prior beliefs about the efficacy of a predictive model, the proposed decision-making strategy for compensation significantly increases the value of a given print to a manufacturer under simulated preferences.

Keywords: Deviation Compensation; Multi-Attribute Utility Theory; 3D Printing; Decision Analysis; CAD

1. Introduction

1.1. Background

One consequence of the increasing use of additive manufacturing (AM) to produce functional parts is a significant need to ensure high dimensional accuracy for printed objects. Unfortunately, a gap still remains between the required accuracy for many applications and the achievable accuracy on many AM machines. A significant amount of work in the literature has been directed towards improving the geometric and dimensional accuracy of 3D printed parts. This research can be divided into several broad fields, the most popular of which include process planning and print process parameter optimization [1–5], online monitoring [6–12], and product design adjustment based on predictive modeling [13–19].

Efforts to optimize a printing process' parameters frequently adopt experimental design approaches to select the process settings that produce parts with the greatest overall accuracy. The parameters to be optimized vary greatly from machine to machine and process to process, thus necessitating a new experiment for each machine model, or when the process is fundamentally changed, i.e. when the software is updated.

Work in the area of online monitoring has sought to capture *in situ* data during a printing process and leverage it to proactively stop processes that are likely to produce poor quality parts, or to trigger actions intended to improve the quality of a part. Examples of a possible action for a laser powder bed fusion (LPBF) process could include remelting a layer or removing a layer with a defect and resuming the print. Process parameters could also be adjusted on the fly.

Finally, approaches utilizing predictive product design adjustment seek to generate predictions for the geometric inaccuracies of a manufactured part, and then adjust the dimensions of the part before printing so as to compensate for them, producing a part with the intended dimensions. Below we provide a detailed review of design adjustment methods.

10.1016/j.promfg.2021.06.038

1.2. Predictive product design adjustment

This approach was utilized by Tong, et al. [13] to improve the accuracy of parts produced using stereolithography (SLA). The proposed process started with a kinematic model designed to predict the dimensional inaccuracies of the printed part caused by inaccuracies in the motion of a mirror that reflects the printer's laser beam into the resin vat. A test artifact was designed, produced, and measured to determine the coefficients in the kinematic model. With the fitted model, Tong, et al. generated predictions for the inaccuracies of a new part that was similar to the test artifact. These predictions were used to modify each vertex in the part's STL file, which is a triangular mesh representation of the 3D shape that is to be printed. This file format is widely used in the field of additive manufacturing. An illustration of such a file is shown in Figure 1. Each vertex in the triangular mesh was translated in the direction opposite to the predicted translation due to kinematic error. A part produced using the compensated STL file was compared to one produced using the original STL file, and was found to have significantly less volumetric error. Tong, et al. [14] then extended this work for use with a fused deposition modeling (FDM) printer by developing a separate kinematic error model for that machine. They further demonstrated the application of compensation to the part's slice file.

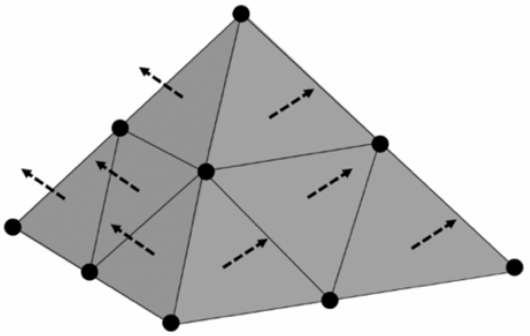

Fig. 1. Simplified illustration of an STL file, including vertices, faces, and normal vectors.

Huang, et al. [15,16,18–20] proposed a strategy to optimally compensate for a part's predicted deformation based on the analysis that a design incorporating compensation might have a slightly different distortion pattern than the original design. The proposed method addresses this by accounting for the predicted additional deviations caused by adding compensation. Huang, et al. employed this compensation strategy along with a parametric function-based predictive modeling approach to generate predictions of geometric errors for 2D freeform shapes [15,16,18] and 3D primitive shapes [19]. Using this method, dimensional accuracy for 2D freeform shapes was shown to increase by fifty percent or more.

Decker, et al. [21] developed a data-driven modeling approach that used past geometric accuracy data from a printer, along with several predictor variables calculated from triangular mesh shape representations of printed parts in order to train a machine learning model. This model was then used to generate predictions of accuracy for new shapes that were to be printed, which were dissimilar to those in the training set. Compensation based on the predictions was applied in a manner similar to Tong, et al. [13], however vertices were translated along the median vector calculated using the adjacent normal vectors to each vertex on the triangular mesh as opposed to utilizing a vertex correspondence approach. This is illustrated in Figure 2. Decker, et al. [21] demonstrated a forty percent improvement of dimensional error for a printed part using training data from different shapes.

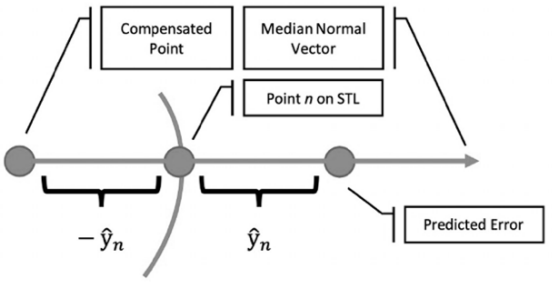

Fig. 2. Compensation strategy used in Decker, et al [21].

Chowdhury, et al. [22,23] used a thermal modeling based approach to predict thermal deformations generated in parts produced using selective laser sintering (SLS). Predictions of distortion from a thermo-mechanical finite element analysis (FEA) model were used to train a neural network. For the network, an instance in the model was a vertex on the part's STL file. During training, the post-deformation positions of vertices were used as predictor variables, and the pre-deformation position of those vertices treated as a response. Once this model was trained, the network was used to predict the proper compensated position of each vertex on a part's designed STL file. This worked by having the neural network predict what staring vertex position would result in the desired vertex position once distortion was added.

McConaha and Anand [24] iterated on this approach, using a sacrificial build instead of a predictive model. Under this strategy, a part is printed and then 3D scanned, with the measured distortions then used instead of predicted distortions. McConaha and Anand used a neural network compensation approach similar to Chowdhury, et al. [22,23], but instead used the post-deformation positions of vertices to train a network that would predict the reverse of vectors describing the transformation between design and deformed points. This was done so as to mitigate issues due to extrapolation.

Zhang, et al. [25] further built on this line of work, and proposed applying the distortion predictions produced using a thermo-mechanical FEA simulation to a non-uniform rational basis spline (NURBS) surface instead of an STL file so as to preserve accuracy.

One unifying theme found in each of the presented works is a desire to most effectively reduce the magnitude of geometric deviations based on the prior belief of the manufacturer as to what these deviations will be. In the literature, this prior belief

can be defined by a predictive model or simply the results of one or several sacrificial parts.

While this is a reasonable and beneficial goal, there are two aspects to these approaches worth considering. First, because all additive manufacturing methods are inherently complex combinations of several physical processes and engineered systems subject to constant variation, no model or sacrificial part will perfectly predict the magnitude of deviations across the surface of a given part. As a result, all predictions come with inherent uncertainty. Further, the effects of compensation itself are subject to natural variations in the printing process. Therefore, knowledge regarding uncertainty of these outcomes would be worth considering when determining when and where to apply compensation. If information regarding how the model performs on previously unseen data is known, it would be desirable that this prior probability distribution influences the compensation that is performed.

Second, not all improvements or reductions in geometric accuracy are equal in the eyes of a manufacturer. A manufacturer might be able to employ a tools such as a grinder, or a hybrid manufacturing system [26] to correct for dimensions that are too large, but unable to correct for dimensions that are too small in post-processing. In this case, inaccurate compensation that produces dimensions that are too small is far more costly than inaccurate compensation producing dimensions that are too large. A manufacturer might also have to meet certain tolerance requirements. In this case, compensation that puts a part within the required tolerances would be far preferable to compensation that leaves or puts the part's dimensions outside of them. Similarly, asymmetric tolerances [27] might be encountered, which could influence the significance of certain compensation errors. Intuitively, an ideal compensation strategy should take these considerations into account.

1.3. Multi-attribute utility theory

One possible tool for performing compensation while incorporating information regarding a method's uncertainty and a manufacturer's preferences is Multi-Attribute Utility Theory (MAUT) [28]. Under this approach, a decision maker starts by constructing a model that ascribes a dollar value to a set of conditions. In this case, these conditions might be the overall accuracy of the print, or whether it is within certain tolerances. Then, a von Neumann-Morgenstern utility is calculated from the given value function and the probability distribution of the various outcomes. The optimal compensation strategy is that which maximizes the expected utility.

Several examples of MAUT being applied to manufacturing decisions exist in the literature. One cluster of work has focused on the application of MAUT and Bayesian analysis to subtractive manufacturing. Abbas, et al. [29] demonstrated the use of decision analysis in order to optimize profit for a manufacturer performing a milling operation. The decisions considered included which tools to use, and which process parameters should be selected. The cost due to tool wear and labor to perform the milling operation were both major parts of this study. Hupman, et al. [30] build on this approach by evaluating the effectiveness of different incentive structures for achieving optimal value for a manufacturer by properly incentivizing milling machine operators. Schmitz, et al. [31] go into greater depth in describing the application of Bayesian analysis for this application while Zapata-Ramos et al. [32] studied the value of information and experimentation in context of efforts to optimize profit. Finally, Karandikar, et al. [33] utilized Bayesian updating to predict tool life in these systems.

Xu and Huang [34] applied MAUT to analyze setup plans in the field of process planning. Their work provided a case study illustrating how to define optimality of a setup plan by combining manufacturing error simulation with MAUT. Pergher and Teixeira de Almeida [35] applied MAUT to choose the proper parameters for a production plan under uncertainty. They later developed a multi-attribute utility model for choosing which dispatching rules to use in a job shop environment [36]. Other methods of decision analysis such as the Analytic Hierarchy Process (AHP) and the weight and rate method have been applied to AM, specifically for decisions related to which AM method or material to use, or which process settings to employ [37–39].

1.4. Scope and contributions

The main contribution of this paper is to propose a methodology by which the efficacy of a compensation strategy for AM can be evaluated given prior beliefs about the model's performance, and a manufacturer's priorities. To our knowledge, no study has reported on the use of decision analysis to support optimal decision-making for a 3D shape compensation strategy in AM. This allows a manufacturer to evaluate whether a given compensation strategy should be employed, or which should be chosen given multiple options. A further benefit of this approach is that the utility to the manufacturer of producing a given part with or without a compensation strategy is calculated as a dollar value. This would aid in determining pricing strategies for both the parts themselves in a job shop setting, and for software and models that enable compensation. The proposed methodology was evaluated on experimental data from [21]. This paper shows that the conventional compensation strategy frequently fails to maximize a manufacturer's utility, and demonstrates how a simple modification to the strategy can greatly increase expected utility of a given compensated print.

The remainder of this paper is structured as follows. First, considerations for constructing a value function describing a manufacturer's preferences are discussed, and example functions are given. Second, a methodology for calculating the expected utility is described. Third, the compensation strategy used in the study is introduced. Finally, results demonstrating the method are given. The proposed strategy is shown to significantly increase the expected utility of a print.

2. Methodology

2.1. Constructing a value function

The first step in the proposed approach is to develop a value function that describes the preferences a manufacturer has for

a specific print. These preference attributes could include the overall accuracy of the part, specific tolerances, and more, and seek to account for the unique challenges and constraints brought on by using additive manufacturing. The value function seeks to express the dollar value to a manufacturer of a completed print as a function of these attributes. One situation where these values and costs are particularly well defined is in the case of an AM service provider. These businesses accept print jobs from a wide range of companies for a predefined price and with prenegotiated quality requirements. These parts are then manufactured by the service provider at a specific cost, and then returned to the customer, ideally at a profit. Several different value functions will be discussed below, which represent only a small fraction of the possible functions that could be utilized to express manufacturer preferences.

The first value function might be used in a situation where a manufacturer must meet certain tolerances, has no ability to fix an out-of-tolerance print, and derives no benefit from improving the accuracy of the part within the tolerances:

$$V_1 = V_{base}\, I_{t_{all}} - C_P \tag{1}$$

V_{base} is the base value of a successful print of the part. For instance, if the manufacturer is a 3D printing service provider, this would be the price paid by a customer for the part, assuming it met the tolerance requirements. $I_{t_{all}}$ is an indicator variable that is equal to one if the required tolerances have been met, and zero otherwise. Here, tolerance requirements are considered met if each dimension on the part is measured to be within the intended dimension plus t_h or minus t_l, the upper and lower tolerance bounds.

Finally, C_P is the cost to manufacture the part, including materials, energy, machine maintenance, etc. It can be seen here that the value of the print is the difference between the benefits and the cost, and will be negative if the print fails to meet the tolerance requirements. In this situation, the part will either be worth all or nothing to the manufacturer depending on whether it meets tolerance requirements. It should be noted that outside meeting tolerances, increasing or decreasing accuracy doesn't financially impact the manufacturer. This reflects the very common case where tolerances are the only geometric quality metric that must be met by a manufacturer in a contract with a customer.

The second value function might be used in a situation where the manufacturer has no tolerance requirements, but is penalized for errors according to a quadratic loss function:

$$V_2 = B_{max} - \alpha \sum_{i=1}^{n} (\|\boldsymbol{x}_i - \widehat{\boldsymbol{x}}_i\|_2)^2 + V_{base} - C_p \tag{2}$$

B_{max} is the maximum additional value over the base value that would be derived from a perfectly accurate part. The second term sums the squares of geometric deviations at each point over each of the n points that are evaluated, and is then multiplied by the scaling term α to determine the accuracy penalty. Error is defined as the Euclidean norm between the measured position of the point $\boldsymbol{x}_n$ and the designed position of the point $\widehat{\boldsymbol{x}}_n$. An absolute value could be used instead of a square of the error terms if that better reflected the manufacturer's preference. It is desirable that the number of points evaluated across the STL file be made uniformly dense through remeshing, and the constant α be set according to n, so as to not bias the calculation. In this instance, the manufacturer no longer has to meet a set of fixed tolerances, but is instead incentivized financially to minimize the overall error with an exponentially increasing penalty for increasing error magnitudes. This might be the case when a part is being built for prototyping and visualization purposes as opposed to functional end-use. The manufacturer would still value a less accurate part to a lower degree, as a low-quality product would be more likely to leave a customer unsatisfied.

Finally, a third value function might be used in a situation where a manufacturer has tolerance requirements, derives no benefit for improving accuracy within the tolerances, and has an ability to fix an out-of-tolerance dimension if it is larger than the design, albeit at a cost:

$$V_3 = V_{base}\, I_{t_l} + \gamma \sum_{i=1}^{n} \left(t_h - max(t_h, \|\boldsymbol{x}_i - \widehat{\boldsymbol{x}}_i\|_2)\right) - C_P \tag{3}$$

I_{t_l} is equal to one if the lower tolerance requirement has been met, and zero otherwise. There is also a cost for physically repairing geometric deviations that are above the upper tolerance t_h, scaled by γ. In this situation, the part is worth nothing to the manufacturer if a given dimension violates the lower tolerance bound, as they can no longer make that dimension larger once the print is completed. In this way, the manufacturer's incentives are similar to those laid out in the first value function. In this situation, however, a deviation resulting in a dimension that is too large can be fixed using some form of subtractive manufacturing, which could be as simple as a bench grinder and as complex as a CNC machine. Because of the cost for these repairs, the incentive to have no dimension fall below the lower tolerances will have to be weighed against the cost of making some too large.

2.2. Determining a proper utility function

Once a function describing the value of a certain outcome has been established, it is necessary to determine the expected utility over that value function. This is because there is uncertainty as to which outcome will materialize, and decision makers may value different situations differently based on the distribution of risk.

In the case of a service provider manufacturing hundreds if not thousands of part orders a day, it might be reasonable to assume that in the case of a single print with a value in the range of ~$10 to $1,000 they follow the delta property [40]:

$$\tilde{y}_\delta = \tilde{y} + \delta \tag{4}$$

Here, $\tilde{y}$ is the greatest amount of money a decision maker would pay for a deal that pays y_1 dollars with probability p and y_2 dollars with probability 1-p. Similarly, $\tilde{y}_\delta$ is the greatest amount of money a decision maker would pay for a deal that pays $y_1 + \delta$ dollars with probability p and $y_2 + \delta$ dollars with probability 1-p. This is illustrated in Figure 3.

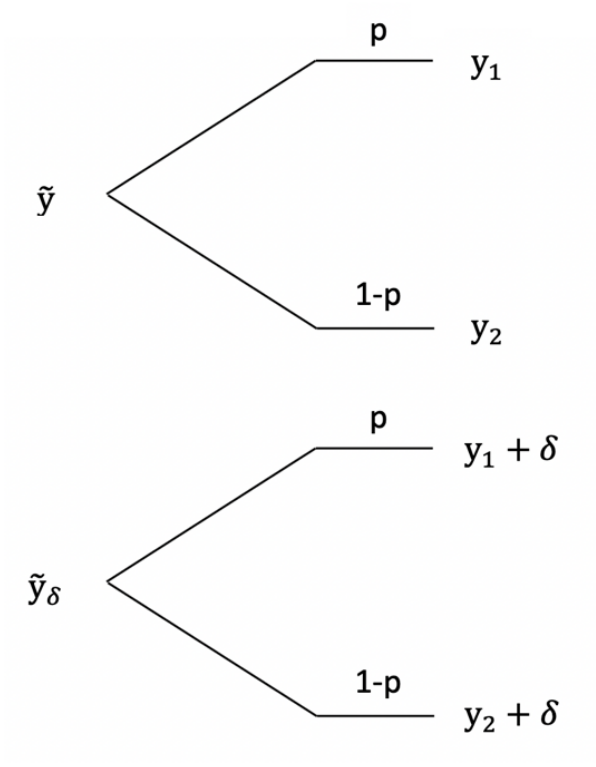

Fig. 3. Lottery modified by shifting the payout.

It might also be reasonable to assume that in the range of ~$10 to $1,000 the manufacturer is risk neutral. This would suggest a linear utility function. As a result, we might determine that a manufacturer's utility is equal to their value function [40]. For this situation, the task of calculating expected utility is greatly simplified. It should be noted that these assumptions will not be reasonable for all manufacturers, especially when the potential value of a part increases significantly. In these cases, a more elaborate utility function will be required.

2.3. Calculating expected utility

With this in place, it is possible to calculate the expected utility of the value functions defined above. The expected utility of the first function becomes

$$E[U(V_1)] = V_{base} P(In\ Tol.) - C_P \quad (5)$$

where $P(In\ Tol.)$ is the probability that all points on the part are within the required tolerances. The expected utility over the second value function can be expressed as:

$$E[U(V_2)] = -\alpha n \int_{-\infty}^{\infty} f_{err}(x)\, x^2 dx + B_{max} + V_{base} - C_P \quad (6)$$

where $f_{err}(x)$ is the probability density function of the prior belief distribution of geometric deviation magnitudes after compensation. Finally, the third expected utility can be expressed as:

$$E[U(V_3)] = V_{base}\, P(In\ Lower\ Tol.) + \gamma\, n \left(t_h - \left(t_h\, F_{err}(t_h) + \int_{t_h}^{\infty} f_{err}(x)\, x\, dx \right) \right) - C_P \quad (7)$$

where $P(In\ Lower\ Tol.)$ is the probability that all points on the part are within the required lower tolerances (not too small). In order to determine each of these expected values, it is necessary to determine $P(In\ Tol.)$, $P(In\ Lower\ Tol.)$, and $f_{err}(x)$. Methodologies for determining these probabilities and distributions will be given in the next two sections.

2.4. Generation of prior belief distributions

The probability density function of the prior belief distribution of geometric deviation magnitudes after compensation $f_{err}(x)$ for this example is empirically generated from a dataset of vertices from a part compensated according to the method proposed in [21]. This reflects the belief of the manufacturer as to the probability of achieving certain magnitudes of vertex deviations on a part compensated using the predictive model and compensation strategy given in [21]. This greatly simplifies the task of understanding uncertainty, since uncertainty regarding the efficacy of predictions, compensation and measurement can all be accounted for in one distribution that focuses on the metric of ultimate interest: deviation. This empirically generated distribution is shown in Figure 4. It can be seen here that this distribution is slightly skewed to the left. Because the distribution is generated empirically, this will cause challenges when determining the joint probability distribution of multiple points, as will be seen later. In an industrial setting, the use of big data analytics would be an enabling technology in this effort, as it would facilitate the collection of large amounts of data representing the efficacy of compensation on individual machines and varying process parameters. This would allow for the use of prior belief distributions that are conditional on the most relevant information available.

2.5. Calculating tolerance probabilities given spatial autocorrelation

Next, it is necessary to determine $P(In\ Tol.)$ and $P(In\ Lower\ Tol.)$ for a new part for which tolerance probabilities are desired based on the data used to generate $f_{err}(x)$. The part will be evaluated at a set of n locations on its surface: $\mathbf{L} = \{\mathbf{l_1}, \mathbf{l_2}, \ldots, \mathbf{l_n}\} \in \mathbb{R}^{n \times 3}$ One challenge faced here is that vertices on the surface of the shape within close proximity of each other will likely exhibit some degree of spatial autocorrelation. This was confirmed for the given dataset using Moran's I test [41]. One way to account for this issue is to only measure points across the surface of the part that are sufficiently separated so as to not be influenced by spatial autocorrelation. A semivariogram of the compensation deviation data is given in Figure 5. It can be seen that after points are roughly 20 mm apart, the effect of spatial autocorrelation becomes negligible. If one wishes to simplify the calculation of these probabilities by assuming independence, all measured points must be greater than this distance apart for this dataset.

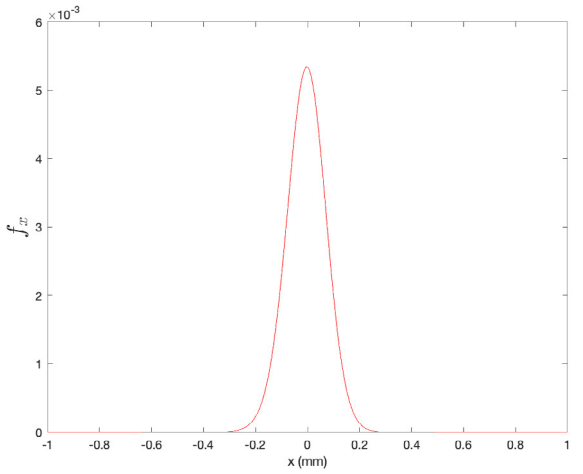

Fig. 4. Probability distribution of geometric deviations of compensated vertices from [21].

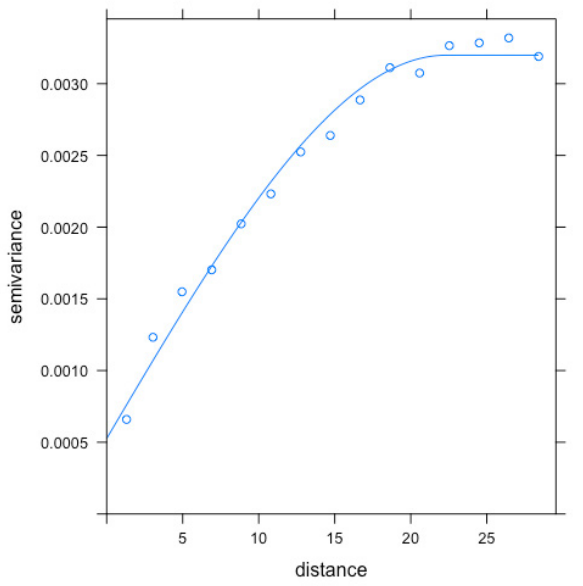

Fig. 5. Semivariogram of the compensation deviation data (mm).

However, it is more likely that the points on the surface of the part that will be measured, often using a coordinate measurement machine or 3D scanner, will be significantly closer than the limit for spatial independence due to their large number (thousands). In this instance, a method for calculating $P(In\ Tol.)$ and $P(In\ Lower\ Tol.)$ while accounting for dependency between the deviation magnitudes of nearby points should be utilized. One will be illustrated below. In it, a Monte Carlo approach is used to determine the percentage of simulated parts that are within and outside of the manufacturer's predefined tolerance requirements, allowing for the determination of $P(In\ Tol.)$ and $P(In\ Lower\ Tol.)$. In order to do this, a large number of sets containing simulated deviations at each of the points to be evaluated on the prospective part are generated and then screened against the manufacturer's predefined tolerancing criteria. For a given set of vertices, it is necessary to draw a random sample of points from the deviation distribution $f_{err}(x)$. However, since the magnitude of deviations at nearby points are dependent on their neighbors, it is necessary to construct and draw magnitudes from a joint probability distribution that takes this correlation into account. This necessitates the simulation of a joint distribution with empirically defined marginals.

One preliminary task that must be done beforehand is to determine the degree of expected covariance between points to be evaluated on the new part to be manufactured. First, functions describing the semivariogram and covariogram are fit to the manufacturer's previous compensation deviation data. These functions seek to describe the relationship between distance between points and covariance for magnitude of deviation. In this example, the spherical variogram model will be utilized, where semivariance γ is a function of distance h given by:

$$\gamma(h;r,s,a) = \begin{cases} 0 & h = 0 \\ a + (s-a)\left(\frac{3h}{2r} - \frac{h^3}{2r^3}\right) & 0 < h \le r \\ s & h > r \end{cases} \quad (8)$$

where a is the nugget of the semivariogram, s is the sill, and r is the range [42]. The spherical covariogram model is given as:

$$C(h;r,s,a) = \begin{cases} s & h = 0 \\ (s-a)\left(1 - \frac{3h}{2r} - \frac{h^3}{2r^3}\right) & 0 < h \le r \\ 0 & h > r \end{cases} \quad (9)$$

These are fit to the compensated deviation data from [21], and shown in Figure 6. Using the spherical covariogram model, it is possible to determine a covariance matrix Σ describing the covariance between each of the points **L** on the part to be evaluated given the distances between them.

With this established, simulated sets of deviation measurements for all of the vertices on the part can be generated by drawing samples from a multivariate distribution with marginals based on the probability distribution $f_{err}(x)$ shown in Figure 4. This can be a challenging task, since $f_{err}(x)$ is an empirical, non-normal distribution. Further, because thousands of points will be evaluated across the surface of the part, the high dimensionality of the data will present an additional hurdle. One useful tool for addressing these challenges is a copula structure, which allows users to describe multivariate joint distributions in terms of univariate marginal distributions and the 'link' between them. In simpler terms, copulas allow for the modeling of dependence between random variables, which is needed for this application. While there are a number of classes of copulas that have been utilized in the literature, one of the more popular copula structures in the Gaussian copula, which is generated from the multivariate normal distribution. Given a correlation matrix $\mathbf{R} \in [-1,1]^{dxd}$ the Gaussian copula can be written as:

$$C_R^{Gauss}(u) = \Phi_R\left(\Phi^{-1}(u_1),\ldots\Phi^{-1}(u_d)\right) \quad (10)$$

where Φ_R is the joint cumulative distribution function (CDF) of the multivariate normal distribution with a mean of zero and covariance matrix corresponding to the correlation matrix R, while Φ^{-1} is the inverse of the CDF of the normal distribution. This structure was chosen because of the flexibility with which it can be used to model complex situations like the one encountered in this application.

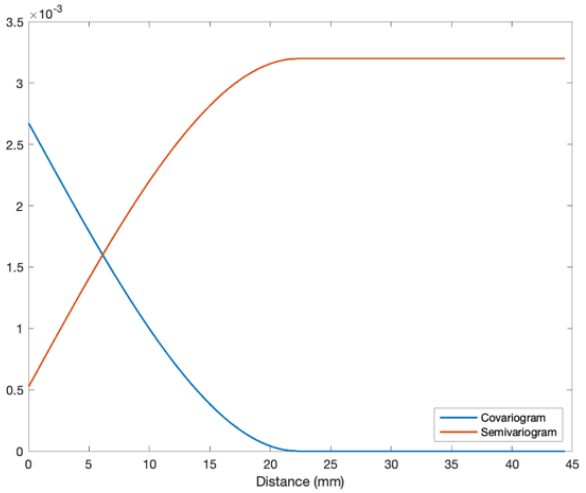

Fig. 6. Semivariogram and covariogram of compensated deviation data.

One method for doing this, which was illustrated in [43] will be utilized here. First, K samples $\boldsymbol{x}_1, \boldsymbol{x}_2, \ldots \boldsymbol{x}_K$ of the n-dimensional vector were generated from a multivariate normal distribution with a covariance matrix Σ. Here, K = 10000 and n = 5000. The cumulative probability of each value is determined using the normal cumulative distribution function $t_{n,i} = \Phi_{k,i}(x_{k,i})$ where k = 1,...,10000 and i = 1,...,5000. Finally, the simulated values of deviation at each evaluated point for each simulated part are generated using the inverse of the cumulative distribution function for the distribution shown in Figure 4: $y_{k,i} = {F_{k,i}}^{-1}(t_{k,i})$. The probabilities $P(In\ Tol.)$and $P(In\ Lower\ Tol.)$ can be determined from the proportion of the generated sets from the multivariate distribution that are entirely within the required tolerances. For the purposes of this work, a part is considered out of tolerance if the deviation at one of its vertices is outside the given constraints, however this same methodology could be applied to other schemes. Once these probabilities are determined, expected utility can be calculated as given in Equations 5-7. It should be noted that one potential downside to the use of Gaussian copulas is their weak tail dependence, which implies that the probability of clusters of extreme events can be underestimated using this approach [44]. It is important that this be weighed against the definition of a part being out of tolerance that is defined by a manufacturer to ensure that the distribution that is described using the copula structure is well suited for estimation.

2.6. Alternative compensation strategy

In order to demonstrate the usefulness of this methodology, a simple alternative compensation strategy is proposed. In this strategy, which is illustrated in Figure 7, each vertex is translated along a vector normal to the surface a distance equal to the opposite of the predicted deviation plus a constant c, which will be the same for every point on the surface of the part. Because $\hat{y}$ will vary for each point, the amount of compensation applied to each point will differ as well. This constant c is simply a parameter of the strategy that will be optimized by choosing the value that maximizes expected utility as calculated using the proposed methodology. The prior belief distribution for the results of the alternative compensation scheme can be approximated by translating the distribution $f_{err}(x)$ by the value c.

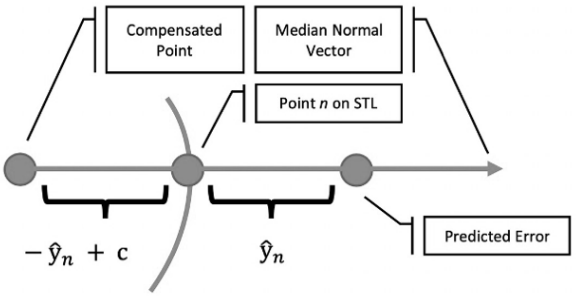

Fig. 7. Alternative compensation strategy.

3. Results

An example scenario is presented below, in order to demonstrate the proposed approach. A manufacturer will build a part, but wishes to employ compensation with an expected distribution of remaining deviations represented in Figure 4. The expected value of the printed part will be evaluated for varying values of the hyperparameter of the compensation strategy c using the three proposed value functions. Parameters for each of the three value functions are chosen in order to reflect a potential situation a manufacturer might face. They are given in Table 1. The expected utility of the compensated part for each value function as a function of different values of c is shown in Figures 8-10. Expected utilities are calculated using the proposed method to account for spatial autocorrelation. The maximum of each function is indicated by a blue circle. It can be seen that in each case, the value of c (mm) that maximizes the expected utility of the compensated part is not zero. The maximum expected utility values using the alternative compensation strategy are compared against the expected utility values from the standard compensation strategy in Table 2.

Table 1. Example parameters for value functions.

Parameter	Value
V_{base}	\$300
C_P	\$100
B_{max}	\$20
t_h	0.225 mm
t_l	- 0.225 mm
α	3
γ	30
n	5000

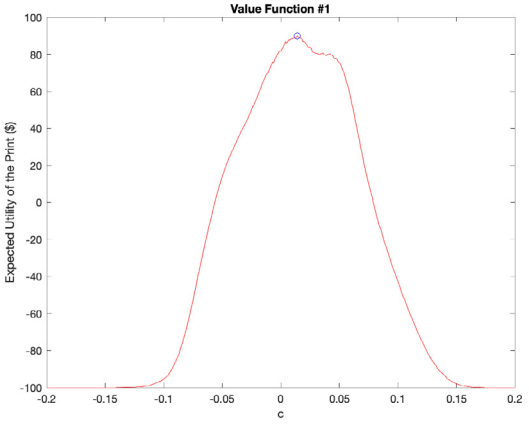

Fig. 8. Expected utility for value function #1 as a function of c.

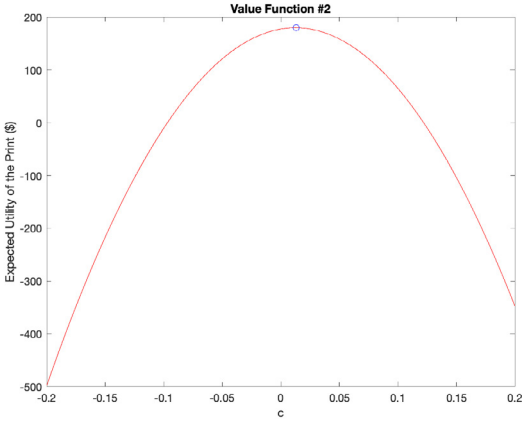

Fig. 9. Expected utility for value function #2 as a function of c.

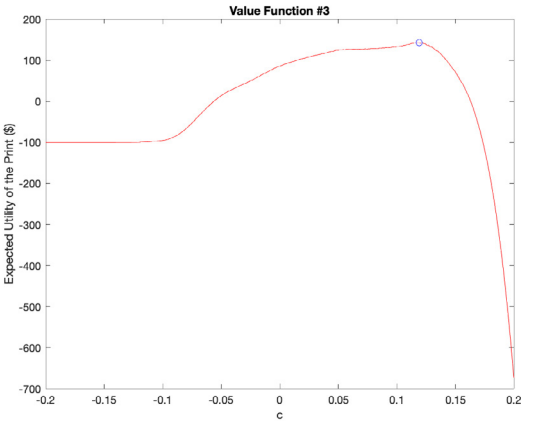

Fig. 10. Expected utility for value function #3 as a function of c.

Table 2. Maximum expected utility.

Value Function	Maximum Expected Utility	Standard Expected Utility (at c = 0)	Difference in Utility Values
#1	\$89.93 (at c = 0.014)	\$81.56	\$8.37
#2	\$179.90 (at c = 0.013)	\$177.50	\$2.40
#3	\$143.30 (at c = 0.119)	\$85.39	\$57.91

Value function #1 simply penalizes prints that are out of the required tolerances, meaning that a value of c that minimizes this likelihood will maximize expected utility. Since the distribution of $f_{err}(x)$ shown in Figure 4 is skewed slightly to the left, we can conclude that the compensation procedure/model utilized in [21] has a slight tendency to produce compensated dimensions that are too small. As a result, a value of c that is positive can help to offset this effect, and thus maximize utility. Similarly, value function #2 is maximized when the overall sum of squares of deviations is minimized. Therefore, the optimal value of c is also positive to account for the skew in $f_{err}(x)$. Finally, value function #3 seeks to keep all absolute deviations above the lower tolerance bound (i.e. no dimensions that are too small) while also minimizing the sum of deviations above the upper tolerance bound (i.e. dimensions that are too large). When c is less than -0.1 mm, the value function flattens out to $-C_P$ as the part is guaranteed to fail the lower tolerance test. When c is greater than -0.1 mm, the likelihood of failing the lower tolerance test decreases, increasing the expected utility. However, as c increases beyond 0.119 mm, the effect of the increasing cost to repair above tolerance deviations outweighs the effect of the decreasing likelihood of lower tolerance failure, and the expected utility decreases rapidly.

Because the value functions are significantly impacted by the manufacturer's preferences, and therefore choice of α and γ, a sensitivity analysis of the two coefficients is useful to determine the generalizability of these results to situations with

differing preferences. Figure 12 illustrates the optimal value of c for value function # 3 as a function of γ. Value function 1 does not utilize α or γ, and is therefore not analyzed here. Since value function #2 only penalizes the sum of squares of deviations, and has no other criteria, the optimal value of c is not sensitive to changes in the α coefficient. We can also see that the optimal value of c for value function #3 is sensitive to the value of γ. This is because increasing cost for repairs on dimensions that are too large causes the optimal value of c to decrease to compensate. Figure 11 illustrates the difference between the maximum expected utility and standard expected utility as a function of α and γ. We can see that this difference increases linearly with α in the case of value function #2 and decreases with increasing γ in the case of value function #3.

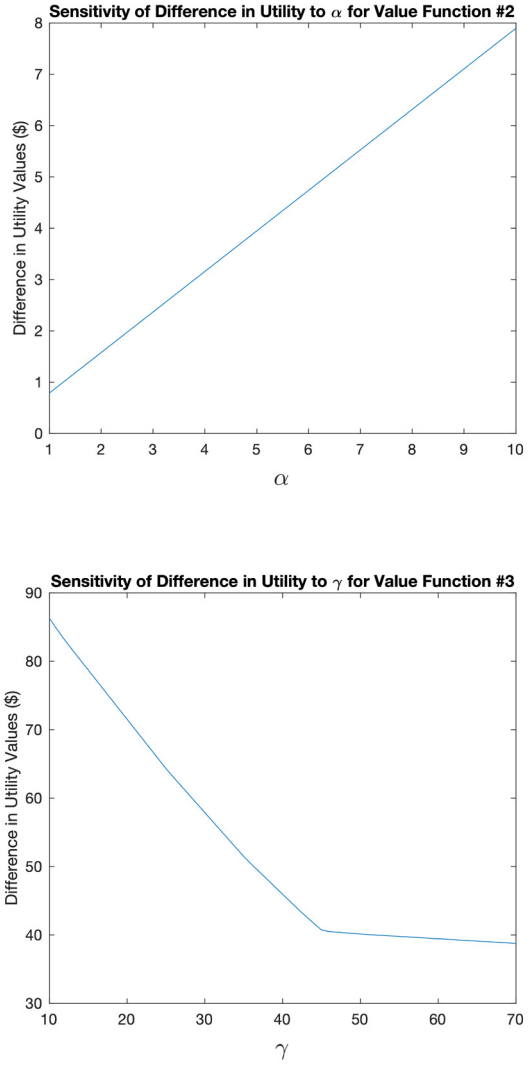

Fig. 11. Sensitivity analysis for the difference in optimal utility values to α and γ for Equations 2 and 3.

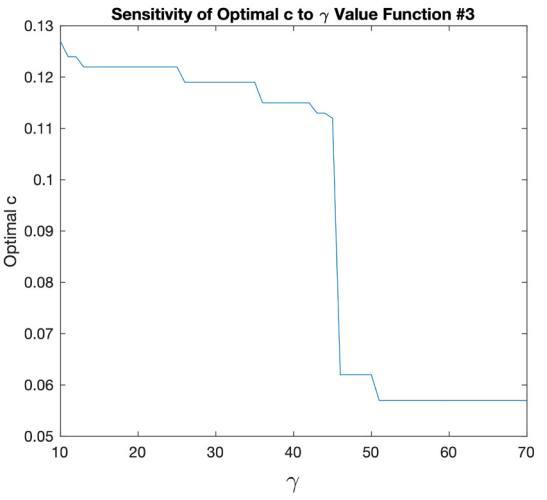

Fig. 12. Sensitivity analysis for the optimal value of c to γ for Equation 3.

4. Conclusion

It can be seen from these results that the conventional compensation strategy, which seeks to minimize a part's deviations, does not necessarily optimize the expected utility of a produced part. Further, even with a relatively simple change to the conventional compensation strategy, it is possible to significantly increase the expected utility of a given print.

Because each manufacturer will have different incentives and tolerance for risks of different magnitudes, the value functions and utility functions determined over the value functions will need to be adjusted accordingly.

This general methodology can also be used for other applications. It could useful for a manufacturer to determine whether they should attempt to print a part on a given machine or with a specific predictive model. It could also be used to help a service provider determine whether it should accept a specific job, or how it should price contracts for prints with certain tolerances and requirements.

There are two limitations to the proposed methodology that should be highlighted. First, the calculations of expected utility are only as accurate as the data they are based on. In the absence of adequate data, or when using deviation data that is not representative of the situation the manufacturer will be facing, recommendations based on this methodology will not be useful. Second, constructing a value function describing a manufacturer's preferences can be difficult. While three different functions that account for relevant outcomes are proposed here, real world value functions can be highly complex, and difficult to pin down. There is a significant body of work that should be consulted on how best to elicit information for constructing a value function while avoiding biases and pitfalls.

Acknowledgements

This research was supported by the National Science Foundation (NSF) under grant CMMI-1901514 and by a graduate research fellowship from the Rose Hills Foundation.

References

[1] Zhang B, Goel A, Ghalsasi O, Anand S. CAD-based design and pre-processing tools for additive manufacturing. J Manuf Syst 2019;52:227–41. https://doi.org/10.1016/j.jmsy.2019.03.005.

[2] Aboutaleb AM, Tschopp MA, Rao PK, Bian L. Multi-Objective Accelerated Process Optimization of Part Geometric Accuracy in Additive Manufacturing. J Manuf Sci Eng 2017;139:101001. https://doi.org/10.1115/1.4037319.

[3] Price S, Cheng B, Lydon J, Cooper K, Chou K. On Process Temperature in Powder-Bed Electron Beam Additive Manufacturing: Process Parameter Effects. J Manuf Sci Eng 2014;136:061019. https://doi.org/10.1115/1.4028485.

[4] Lanzotti A, Martorelli M, Staiano G. Understanding Process Parameter Effects of RepRap Open-Source Three-Dimensional Printers Through a Design of Experiments Approach. J Manuf Sci Eng 2015;137:011017. https://doi.org/10.1115/1.4029045.

[5] Mohamed OA, Masood SH, Bhowmik JL. Optimization of fused deposition modeling process parameters: a review of current research and future prospects. Adv Manuf 2015;3:42–53. https://doi.org/10.1007/s40436-014-0097-7.

[6] Li Z, Liu X, Wen S, He P, Zhong K, Wei Q, et al. In situ 3D monitoring of geometric signatures in the powder-bed-fusion additive manufacturing process via vision sensing methods. Sensors (Switzerland) 2018;18. https://doi.org/10.3390/s18041180.

[7] Montazeri M, Rao P. Sensor-Based Build Condition Monitoring in Laser Powder Bed Fusion Additive Manufacturing Process Using a Spectral Graph Theoretic Approach. J Manuf Sci Eng 2018;140:091002. https://doi.org/10.1115/1.4040264.

[8] Everton SK, Hirsch M, Stavroulakis PI, Leach RK, Clare AT. Review of in-situ process monitoring and in-situ metrology for metal additive manufacturing. Mater Des 2016;95:431–45. https://doi.org/10.1016/j.matdes.2016.01.099.

[9] Grasso M, Valsecchi G, Colosimo BM. Powder bed irregularity and hot-spot detection in electron beam melting by means of in-situ video imaging. Manuf Lett 2020;24:47–51. https://doi.org/10.1016/j.mfglet.2020.03.011.

[10] Lu Y, Wang Y. Monitoring temperature in additive manufacturing with physics-based compressive sensing. J Manuf Syst 2018;48:60–70. https://doi.org/10.1016/j.jmsy.2018.05.010.

[11] Jafari-Marandi R, Khanzadeh M, Tian W, Smith B, Bian L. From in-situ monitoring toward high-throughput process control: cost-driven decision-making framework for laser-based additive manufacturing. J Manuf Syst 2019;51:29–41. https://doi.org/10.1016/j.jmsy.2019.02.005.

[12] Liu C, Law ACC, Roberson D, Kong Z (James). Image analysis-based closed loop quality control for additive manufacturing with fused filament fabrication. J Manuf Syst 2019;51:75–86. https://doi.org/10.1016/j.jmsy.2019.04.002.

[13] Tong K, Lehtihet EA, Joshi S. Software compensation of rapid prototyping machines. Precis Eng 2004;28:280–92. https://doi.org/10.1016/j.precisioneng.2003.11.003.

[14] Tong K, Joshi S, Lehtihet EA. Error compensation for fused deposition modeling (FDM) machine by correcting slice files. Rapid Prototyp J 2008;14:4–14. https://doi.org/10.1108/13552540810841517.

[15] Huang Q, Zhang J, Sabbaghi A, Dasgupta T. Optimal offline compensation of shape shrinkage for three-dimensional printing processes. IIE Trans (Institute Ind Eng 2015;47:431–41. https://doi.org/10.1080/0740817X.2014.955599.

[16] Huang Q. An Analytical Foundation for Optimal Compensation of Three-Dimensional Shape Deformation in Additive Manufacturing. J Manuf Sci Eng 2016;138:061010. https://doi.org/10.1115/1.4032220.

[17] Wang A, Song S, Huang Q, Tsung F. In-Plane Shape-Deviation Modeling and Compensation for Fused Deposition Modeling Processes. IEEE Trans Autom Sci Eng 2017;14:968–76. https://doi.org/10.1109/TASE.2016.2544941.

[18] Huang Q, Nouri H, Xu K, Chen Y, Sosina S, Dasgupta T. Statistical Predictive Modeling and Compensation of Geometric Deviations of Three-Dimensional Printed Products. J Manuf Sci Eng 2014;136:061008. https://doi.org/10.1115/1.4028510.

[19] Huang Q, Wang Y, Lyu M, Lin W. Shape Deviation Generator (SDG) - A Convolution Framework for Learning and Predicting 3D Printing Shape Accuracy. IEEE Trans Autom Sci Eng 2020;17:1486–500. https://doi.org/10.1109/TASE.2019.2959211.

[20] Luan H, Huang Q. Prescriptive Modeling and Compensation of In-Plane Shape Deformation for 3-D Printed Freeform Products. IEEE Trans Autom Sci Eng 2017;14:73–82.

[21] Decker N, Lyu M, Wang Y, Huang Q. Geometric Accuracy Prediction and Improvement for Additive Manufacturing Using Triangular Mesh Shape Data. J Manuf Sci Eng 2021;143. https://doi.org/10.1115/1.4049089.

[22] Chowdhury S, Anand S. Artificial Neural Network Based Geometric Compensation for Thermal Deformation in Additive Manufacturing Processes. Proc. ASME MSEC, June 27 - July 1, 2016, Blacksburg, Virginia, USA: 2016, p. MSEC2016-8784, p. V003T08A006. https://doi.org/10.1115/MSEC2016-8784.

[23] Chowdhury S, Mhapsekar K, Anand S. Part Build Orientation Optimization and Neural Network-Based Geometry Compensation for Additive Manufacturing Process. J Manuf Sci Eng 2018;140:031009-1-031009–15. https://doi.org/10.1115/1.4038293.

[24] McConaha M, Anand S. Additive manufacturing distortion compensation based on scan data of built geometry. J Manuf Sci Eng Trans ASME 2020;142:1–14. https://doi.org/10.1115/1.4046505.

[25] Zhang B, Li L, Anand S. Distortion Prediction and NURBS Based Geometry Compensation for Reducing Part Errors in Additive Manufacturing. Procedia Manuf 2020;48:706–17. https://doi.org/10.1016/j.promfg.2020.05.103.

[26] Manogharan G, Wysk R, Harrysson O, Aman R. AIMS - A Metal Additive-hybrid Manufacturing System: System Architecture and Attributes. Procedia Manuf 2015;1:273–86. https://doi.org/10.1016/j.promfg.2015.09.021.

[27] Maghsoodloo S, Li MH. Optimal asymmetric tolerance design. IIE Trans (Institute Ind Eng 2000;32:1127–37. https://doi.org/10.1080/07408170008967467.

[28] von Neumann J, Morgenstern O. Theory of games and economic behavior. Princeton, NJ: Princeton University Press; 1944. https://doi.org/10.1090/s0273-0979-99-00832-0.

[29] Abbas AE, Yang L, Zapata R, Schmitz TL. Application of decision analysis to milling profit maximisation: An introduction. Int J

Mater Prod Technol 2009;35:64–88. https://doi.org/10.1504/IJMPT.2009.025220.

[30] Hupman AC, Abbas AE, Schmitz TL. Incentives versus value in manufacturing systems: An application to high-speed milling. J Manuf Syst 2015;36:20–6. https://doi.org/10.1016/j.jmsy.2015.02.004.

[31] Schmitz TL, Karandikar J, Ho Kim N, Abbas A. Uncertainty in machining: Workshop summary and contributions. J Manuf Sci Eng Trans ASME 2011;133. https://doi.org/10.1115/1.4004923.

[32] Zapata-Ramos RE, Schmitz TL, Traverso M, Abbas A. Value of information and experimentation in milling profit optimisation. Int J Mechatronics Manuf Syst 2009;2:580–99. https://doi.org/10.1504/ijmms.2009.028082.

[33] Karandikar JM, Abbas AE, Schmitz TL. Tool life prediction using Bayesian updating. Part 1: Milling tool life model using a discrete grid method. Precis Eng 2014;38:18–27. https://doi.org/10.1016/j.precisioneng.2013.06.006.

[34] Xu N, Huang SH. Multiple attributes utility analysis in setup plan evaluation. J Manuf Sci Eng Trans ASME 2006;128:220–7. https://doi.org/10.1115/1.2117407.

[35] Pergher I, de Almeida AT. A multi-attribute decision model for setting production planning parameters. J Manuf Syst 2017;42:224–32. https://doi.org/10.1016/j.jmsy.2016.12.012.

[36] Pergher I, de Almeida AT. A multi-attribute, rank-dependent utility model for selecting dispatching rules. J Manuf Syst 2018;46:264–71. https://doi.org/10.1016/j.jmsy.2018.01.007.

[37] Zaman UK uz, Rivette M, Siadat A, Mousavi SM. Integrated product-process design: Material and manufacturing process selection for additive manufacturing using multi-criteria decision making. Robot Comput Integr Manuf 2018;51:169–80. https://doi.org/10.1016/j.rcim.2017.12.005.

[38] Wang Y, Blache R, Xu X. Selection of additive manufacturing processes. Rapid Prototyp J 2017;23:434–47. https://doi.org/10.1108/RPJ-09-2015-0123.

[39] Zhang Y, Bernard A. An integrated decision-making model for multi-attributes decision-making (MADM) problems in additive manufacturing process planning. Rapid Prototyp J 2014;20:377–89. https://doi.org/10.1108/RPJ-01-2013-0009.

[40] Abbas A. Foundations of Multiattribute Utility. 1st ed. Cambridge University Press; 2018.

[41] Moran P. Notes on Continuous Stochastic Phenomena. Biometrika 1950;37:17–23.

[42] Smith TE. Notebook on Spatial Data Analysis n.d. http://www.seas.upenn.edu/~ese502/#notebook (accessed August 24, 2020).

[43] Wang T, Dyer JS. A copulas-based approach to modeling dependence in decision trees. Oper Res 2012;60:225–42. https://doi.org/10.1287/opre.1110.1004.

[44] Furman E, Kuznetsov A, Su J, Zitikis R. Tail dependence of the Gaussian copula revisited. Insur Math Econ 2016;69:97–103. https://doi.org/10.1016/j.insmatheco.2016.04.009.